ELSEVIER

Journal of Organometallic Chemistry 657 (2002) 20–39

Journal of Organometallic Chemistry

www.elsevier.com/locate/jorganchem

The use of Kitaigorodskii's *Aufbau* principle in the solid-state study of crystalline borane compounds. A preliminary account

Caroline O'Dowd [1], John D. Kennedy, Mark Thornton-Pett *

The Borane and The Crystallographic Research Laboratories, The School of Chemistry of the University of Leeds, Leeds LS2 9JT, UK

Received 15 October 2001; accepted 7 May 2002

Abstract

Very many molecular structures of polyhedral borane compounds have been established by solid-state crystallographic analysis, but their intermolecular interactions, and the factors that dictate their supramolecular arrangements in the crystal lattice, are essentially unexamined. Kitaigorodskii's *Aufbau* principle (KAP) forms the basis of a technique for such an examination and simplifies the visualisation of molecular packing by breaking it down into a series of symmetry-generated steps, of which each permits even the weakest intermolecular interactions to be readily identified. KAP is based on close-packing principles, and constructs the crystal of a molecular compound in a three-step process: first, the molecular units pack to form one-dimensional chain substructures, these then pack together to yield two-dimensional sheet substructures; these, in turn, stack on top of one another to yield the observed three-dimensional structure. The method is exemplified by consideration of the molecular arrangements in the 'wrap-around' encapsulation of 4,4′-bipyridyl with [6,9-(4,4′-bipyridyl)$_2$-*arachno*-$B_{10}H_{12}$] in their 1:1 co-crystal, the complex three-dimensional dihydrogen-bonding network in the crystal structure of H_3BNH_3, solvent channels in the structure of the co-crystal of *n*-hexane with [C_5H_5NMe][1-(SMe)-10-(SMe_2)-*closo*-$B_{10}H_8$], and systematic variations within the crystal structures of [6,9-(NC_5H_4-4-R)$_2$-*arachno*-$B_{10}H_{12}$], where R is Me, Et and *n*-Pr. It is concluded in this preliminary account that KAP provides a simple yet rigorous tool for studying a whole range of both gross and subtle molecular packing effects in the solid-state. © 2002 Published by Elsevier Science B.V.

Keywords: Structural systematics; Crystal engineering; Supramolecular; Close-packing; Kitaigorodskii's *Aufbau* principle; Borane cluster compounds; Weak intermolecular interactions; Dihydrogen-bonding

1. Introduction

In the structural investigation of molecular polyhedral boron-containing cluster chemistry by single-crystal X-ray diffraction analysis, it has been generally conventional to confine the structural interpretation to the individual molecules. Thus when a molecular structure as determined by single-crystal X-ray work is presented, it is presented typically as a ball-and-stick picture of the molecule as if it were a molecule of a gas, independent of its environment in an extended solid-state matrix. Specific solid-state features that can be of high chemical and structural significance, including fascinating assembly phenomena arising from a variety of attractive intermolecular interactions, are often overlooked. Polyhedral boron-containing cluster compounds generally consist of irregularly shaped molecules that give rise to complicated solid-state packing arrangements that are often characterised by extensive networks of weaker intermolecular attractions. These can include, for example, XH···π interactions, CH···HB and NH···HB 'dihydrogen' bonding, and so on, in addition to more familiar intramolecular interactions such as conventional X–H···X hydrogen-bonding and van der Waals attractions. The nature of these types of interactions and their relative contributions to the assembly of molecules in the crystalline state are, however, as yet poorly understood, and boron-containing cluster chemistry is no exception here. The balance of these forces dictates patterns among a whole variety of solid-state phenomena [1], and those that we have started to examine in our laboratories include: (a) crystal polymorphism; (b)

* Corresponding author
E-mail address: marktp@chem.leeds.ac.uk (M. Thornton-Pett).
[1] Formerly Caroline Price, Refs. [10–14,26]

0022-328X/02/$ - see front matter © 2002 Published by Elsevier Science B.V.
PII: S0022-328X(02)01587-5

mixed-molecule chemistry, as in solvates or co-crystals; (c) aggregation into 'counter-intuitively' localised layers or channels in ionic salts involving polyhedral boron-containing cluster anions species; (d) supramolecular assemblies such as rods, helices, tapes, capsules, sheets, and so on. These structural features are specific to the solid-state. Together, they can lead to the pursuit of ideas that (e) systematic comparisons of closely related structures can ultimately lead to the introduction of specific solid-state features by design [2].

In order to identify these solid-state phenomena and then examine comparatively, systematically, and rigorously, our intent is to adopt a universal approach that can be applied to all of them because a mixture of several different procedures could lead to confusion. Methods for the analysis of solid-state structures do, of course, exist. For example, the systematic description of intermolecular hydrogen-bonding networks using graph set notation [3,4]. Such approaches are not generally adopted because they do not necessarily aid chemical understanding and can, in some cases, add unnecessary complexity. Rather, the general approach to identification and delineation of intermolecular aspects of the solid-state of molecular compounds has been hitherto more random. Studies are often limited to the display of a packing diagram of a set of molecules in the crystal lattice, from a perspective chosen to show a perceived clear view. This view is then interpreted in terms of a perceived particular feature of interest for the compound under study. This approach is not always satisfactory, either from the point of view of the detailed comparison of series of related structures, or from the point of view of objectively assessing all the significant features of intermolecular interaction.

In this essentially preliminary presentation we enunciate an alternative method for the systematic analysis of the solid-state packing of boron containing cluster compounds. This is based on Kitaigorodskii's *Aufbau* Principle (KAP) [5]. Four examples are chosen to illustrate the simplicity and versatility of the method. We believe that these examples demonstrate that KAP forms the basis of a useful visual tool for the analysis and delineation of a wide range of solid-state phenomena regardless of molecular size and complexity. The emphasis is on KAP as a method of analysis, using diverse systems as examples. We hope to present its detailed application to aspects of comparative crystallography of borane species in due course.

2. Kitaigorodskii's *Aufbau* principle

The systematic approach we assess here for the comparative assessment of intermolecular behaviour in boron-containing cluster chemistry has its roots in the simple inorganic solid-state chemistry of simple binary and ternary salts and ceramics. For such species, it is generally well recognised that a very small number of structural types, e.g. caesium chloride, rock salt, nickel arsenide, sphalerite, wurtzite, etc. describe many thousands of different compounds [6]. This arises because these compounds adopt close-packed layers of anions, and the natural limits of the relative sizes and ratios among the ions can dictate only a relatively small number of lattice arrangements.

Table 1
The 11 most populous space groups [a]

Space group	Number (%)
$P2_1/c$	86 573 (35.3)
$P\bar{1}$	50 532 (20.7)
$P2_12_12_1$	21 152 (8.6)
$C2/c$	18 233 (7.4)
$P2_1$	13 718 (5.6)
Pbca	9008 (3.7)
$Pna2_1$	3656 (1.6)
Pnma	3560 (1.5)
Cc	2525 (1.0)
P_1	2232 (0.9)
Pbcn	2181 (0.9)

[a] Calculated from 245 393 entries in October 2001 release of the Cambridge structural database [7].

A related phenomenon occurs for crystals of molecular compounds (Table 1). The majority of molecular compounds for which determined crystal structures have been reported crystallise in only a small number of space groups, with only six of the 230 possible space groups accounting for over 80% of all published structures [7]. This is because crystals of molecular compounds in those particular space groups resemble the simple binary and ternary inorganic crystals in that the molecules also generally attempt to close-pack [5]. Consequently, in the crystal structure, a molecule will typically be surrounded laterally by six other molecules, generally in a sheet. Those sheets can then in turn close-pack together to form the observed crystal structure. The way in which the molecules arrange themselves in sheets is manifested in the symmetries of those few space groups (Table 1). It is only those particular space groups that have the combinations of symmetry elements that permit the close-packing, rather than other assemblies, of a set of identical molecules of otherwise random shape and orientation.

The corollary of these considerations is that the overall three-dimensional crystal structure of a molecular compound can be broken down into a series of 'two-dimensional' layers of laterally close-packed molecules, and that those layers relate to one another, and stack together, using a specific symmetry element of the space group concerned. These close-packed layers can thence be interpreted similarly in terms of a series of close-

packed 'one-dimensional' chain substructures, which pack to form the two-dimensional layers using another specific symmetry element inherent to that space group. Finally, the chain substructures consist of series of individual molecules related successively by symmetry operations that are again necessarily from within that space group. In sum, the structure of the crystal of a molecular compound can be broken down systematically into layers, and then chains, and then finally the molecule itself [8,9].

The approach for the analysis of intermolecular interactions is one that essentially inverts this procedure. Thus, firstly, it delineates how the molecules come together to build up the quasi-one-dimensional chain substructures, how these then build up into two-dimensional layers, and finally how the layers assemble to generate the observed overall three-dimensional crystal structure. This approach was pioneered by Kitaigorodskii half a century ago [5], and is referred to as Kitaigorodskii's *Aufbau* principle, conveniently abbreviated as KAP [8,9]. For the polyhedral boron-containing cluster systems illustrated in this presentation, KAP permits the systematic analysis of the interactions that are involved at each of the individual one-, two- and three-dimensional assembly stages [10–14].

At first sight there would naively appear to be a choice among very many possible one-dimensional chain substructure symmetries that have to be considered, with 75 being in principle possible [15]. This would then, in principle, engender an even larger number of two-dimensional sheet structures. However, when the symmetry constraints inherent in the most commonly encountered crystal systems are combined with other close-packing considerations, only the four types of close-packed chain substructure need to be invoked in the analysis of most crystalline molecular compounds [16]. These are shown in Fig. 1. Similarly, the 80 possible symmetry-generated sheet structures associated with those four chain structures reduce down only to seven when close-packing considerations are applied [8,17]. KAP can therefore be used quite simply when applied to any of that majority of molecular species that crystallise in the most populous space groups. The method builds up one of these four chain structures from the individual molecules: a second symmetry operation is then applied to develop the chain structure into one of the seven sheet structures, and these sheet sub-structures are then

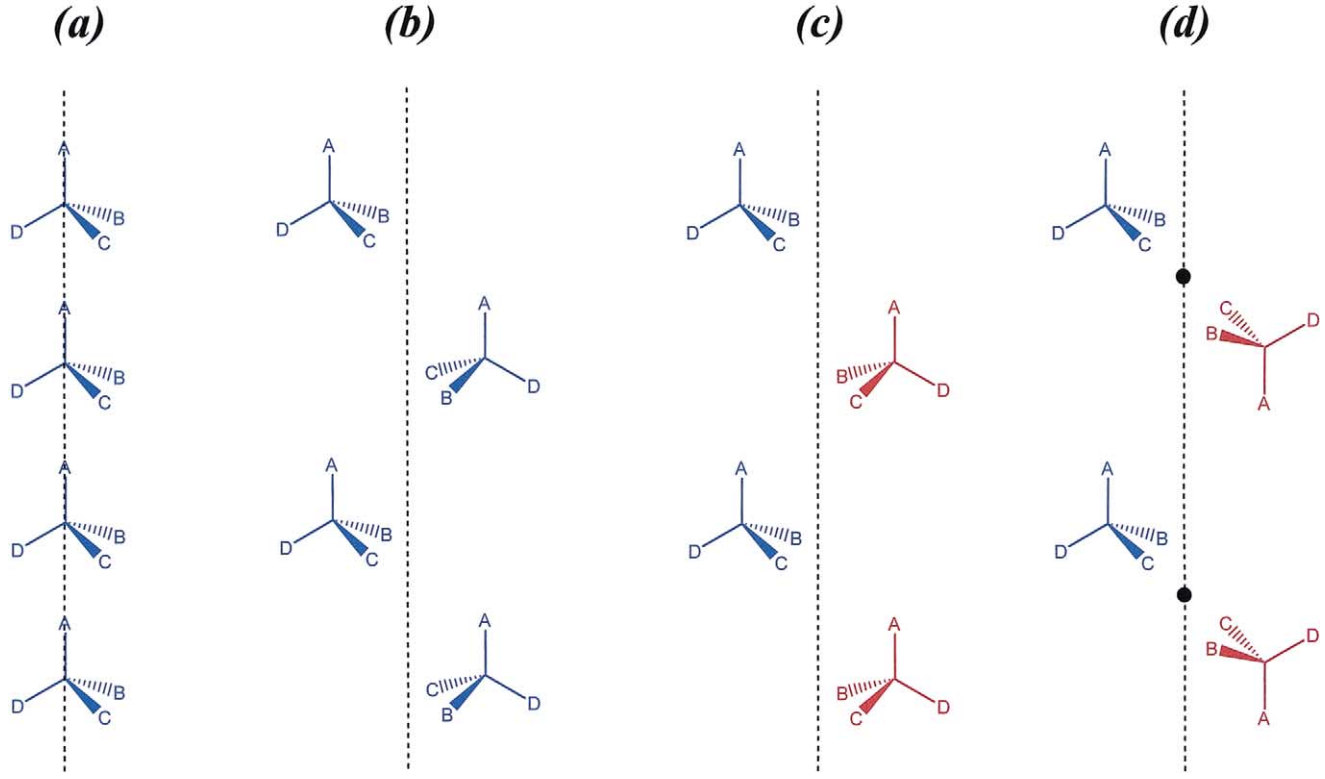

Fig. 1. The four most commonly encountered KAP chain structures: (a) translation; (b) screw; (c) glide; and (d) inversion chains. The respective symmetry operations have been successively applied to a chiral tetrahedral molecule for which the starting absolute configuration is coloured blue and the opposite enantiomer coloured red. The colour scheme clearly shows that, whilst chirality is retained in the chain, as in structures (a) and (b), the symmetry operations of (c) and (d) result in chains of racemates.

assembled to engender the full crystal by a third symmetry operation. At each stage the molecular interactions are inherently displayed and may be examined. Conversely, it is often possible to choose particular directions of chains and sheets and their required symmetry operations in accord with particular intermolecular interactions that may be of interest.

The simplest chain structure is the translational chain (Fig. 1a) in which a molecule is repeatedly moved laterally in a one-unit translation. In the 2_1 screw chain (Fig. 1b) the molecule is rotated by 180° and translated by a half-unit, then again rotated by 180° and translated by a half-unit, and so on. It may be noted that two successive 2_1 screw operations are equivalent to one unit translation of the molecule, and that both the simple translation and screw chain structures imply retention of any molecular chirality. The third type of chain substructure involves a glide operation (Fig. 1c), in which the molecule is reflected across a mirror plane, then translated by half a unit, reflected again across the mirror plane, translated further by half a unit, and so on. This is similar to the screw-chain in that two successive operations are equivalent to one translational chain operation. However, it does differ in that there is an alternation of chirality along the chain. The fourth type of chain is generated by a sequence of successive inversions (Fig. 1d). This is somewhat different to the other three in that this chain is constructed using point-symmetry operations, whereas the other three involve translational symmetry operations. In this fourth type of chain, a molecule is inverted across a centre of symmetry; successive centres of symmetry along the relevant vector direction then develop the chain. This chain also dictates an alternation of molecular chirality.

In sum, therefore, if a molecular structure crystallises in one of the most populous space groups, then close-packing principles can be applied, and the molecular packing can be rigorously described in terms of a simple three-stage *Aufbau* process. Firstly, one of the four chain structures [8,16] in Fig. 1 is constructed by successively applying the relevant symmetry operation to the repeating molecular unit. Next, one of the seven close-packed sheet structures [8,17] is generated, again by successively applying another of the symmetry operations that define the four chain substructures of Fig. 1. Finally, the full three-dimensional macro-structure is generated by applying a third symmetry operation, such that the sheets close-pack one on top of another.

These considerations of symmetry and construction are here illustrated in four specific applications of the KAP method. Each example illustrates different solid-state features so that it can be seen how each can be described and delineated by KAP. The intent is not to produce any unifying solid-state structural overview but rather to exemplify the versatility and simplicity of the KAP method regardless of the system or feature studied. The first example exemplifies the mechanics of the method and also illustrates how it can readily identify intermolecular contacts whilst providing a simple delineation of the macromolecular architecture of an interesting co-crystal. The second example enables the visualisation of the complicated three-dimensional network of bifurcated intermolecular 'dihydrogen' bonds in ammonia borane, H_3NBH_3. The analysis of the $[C_5H_5NMe]^+[1\text{-}(SMe)\text{-}10\text{-}(SMe_2)\text{-}closo\text{-}B_{10}H_8]^-$ salt then permits the identification and description of a subtle network of weak CH···S hydrogen bonds that frames a series of parallel hydrophobic helical channels. The fourth example illustrates the systematic analysis of a series of very closely related species, thereby better enabling the identification of subtle trends.

3. Application of the KAP method to specific examples

3.1. The structure of the 1:1 co-crystal of 4,4′-bipyridyl and [6,9-(4,4′-bipyridyl)$_2$-arachno-B$_{10}$H$_{12}$]

This first example is the co-crystal of [6,9-(4,4′-bipy)$_2$-*arachno*-$B_{10}H_{12}$] (Fig. 2, lower diagram) with 4,4′-bipyridyl (CCDC deposition no. 172365). The [6,9-L_2-*arachno*-$B_{10}H_{12}$] system constitutes an easily synthesisable set of compounds [18] (Fig. 2, upper scheme) with which systematically to engender and examine for subtle variations in intermolecular phenomena of potential wider import in boron-containing cluster chemistry (see also Example 4 below). It also thereby can be usefully used to consolidate the general technique for the application of the KAP method in the general area [10,11,14].

The crystallographic space group is $P2_1/n$. The KAP operations to generate the observed crystal structure must obviously involve both molecules. It is convenient in the KAP approach to start with a molecule of interest as close to the origin as possible, and here the boron-containing molecule can be selected for this role (Fig. 3, upper diagram). Having done this, the co-crystallising free 4,4′-bipyridyl molecule is then most sensibly positioned close to the [6,9-(4,4′-bipyridyl)$_2$-*arachno*-$B_{10}H_{12}$] molecule to make an appropriate bimolecular unit for subsequent KAP chain development (Fig. 3, upper diagram). Incidentally, even in this preliminary step of the analysis, it is of significant chemical and structural interest to note from Fig. 3 that the aromatic rings of the two molecules in the co-crystal pack very neatly next to each other. In this context, see also Example 4 below. There are two inversion centres very close to this bimolecular unit, at (0, 0, 0) and ($\frac{1}{2}$, 0, $\frac{1}{2}$). An inversion chain (Fig. 1d above) is thence readily generated by successive inversions along [101] direction (Fig. 3,

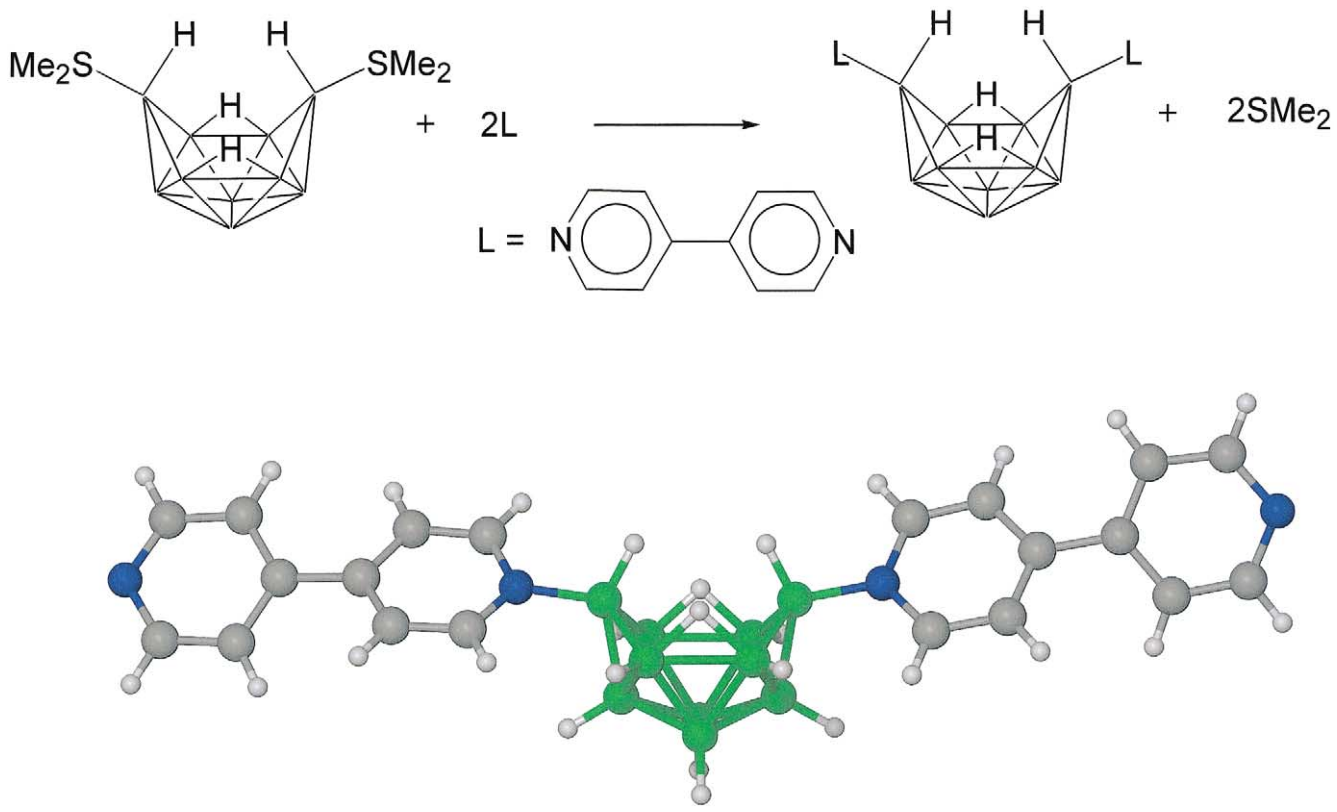

Fig. 2. The general scheme for the synthesis of 6,9-disubstituted *arachno*-decaboranyl compounds (upper scheme) and the molecular structure of [6,9-(4,4′-bipyridiyl)$_2$-*arachno*-$B_{10}H_{12}$] (lower diagram).

middle diagram).[2] It should be noted that each inversion operation further extends the parallel packing of aromatic rings to include four molecules. The next step, to generate the KAP two-dimensional sheet, can then be accomplished by successive 2_1 screw-axis operations along the crystallographic *b*-direction (Fig. 3, lower diagram). This sheet molecular assembly in the [101] plane may seem initially confusing. However, by the removal from the representation of some of the peripheral molecules, and by distinguishing the free 4,4′-bipyridyl co-crystallite by drawing its molecules with atoms sized according to their van der Waals radii whilst drawing the [6,9-(4,4′-bipy)$_2$-*arachno*-$B_{10}H_{12}$] molecules as stick-representations, important structural features become much more readily apparent (Fig. 4, upper diagram). It is thence readily seen that pairs of the co-crystallising 4,4′-bipyridyl molecules are 'walled-in' by four [6,9-(4,4′-bipy)$_2$-*arachno*-$B_{10}H_{12}$] molecules. However, it is not clear from this two-dimensional sheet substructure whether each pair of co-crystallising molecules exists as an isolated unit in its own 'pocket' or whether extended chains develop.

It is therefore of further interest to see how this feature develops in three dimensions. Fig. 4 (middle diagram) shows the orthogonal view of the sheet substructure, i.e. the view in the crystallographic [101] plane. The third KAP step, the final generation of all the structural features of the macroscopic crystal, is thence accomplished by successive unit translations in the crystallographic *a*-direction (Fig. 4, lower diagram). This last diagram reveals that the architecture of the co-crystallising molecules exhibits a 'wrap-around' complexation: double columns of closely-contacting 4,4′-bipyridyl molecules along the crystallographic *a*-axis are encapsulated and surrounded by encompassing [6,9-(4,4′-bipy)$_2$-*arachno*-$B_{10}H_{12}$] molecules. Conversely, the structure can be regarded as based on channels along the *a*-axis within a relatively open lattice of [6,9-(4,4′-bipy)$_2$-*arachno*-$B_{10}H_{12}$] molecules, with the channels being filled by the 4,4′-bipyridyl molecules which thereby form columns. Both descriptions have different chemical implications, but, as far as the molecules are concerned, these two views of the structure are mutually equivalent. Another example of a channel structure is in Example 3 below. In sum, this analysis demonstrates an application of KAP readily revealing how the different molecular species in co-crystals may lie together, and how inter-

[2] Note that, in a rigorously formal KAP approach [5,9,11] this 'first step' would be referred to as 'stage 2', stage 1 being the definition of the repeating molecular unit, or, in some cases, repeating groups of molecules, or in some cases of symmetry, a repeating unit consisting of a fragment of a molecule.

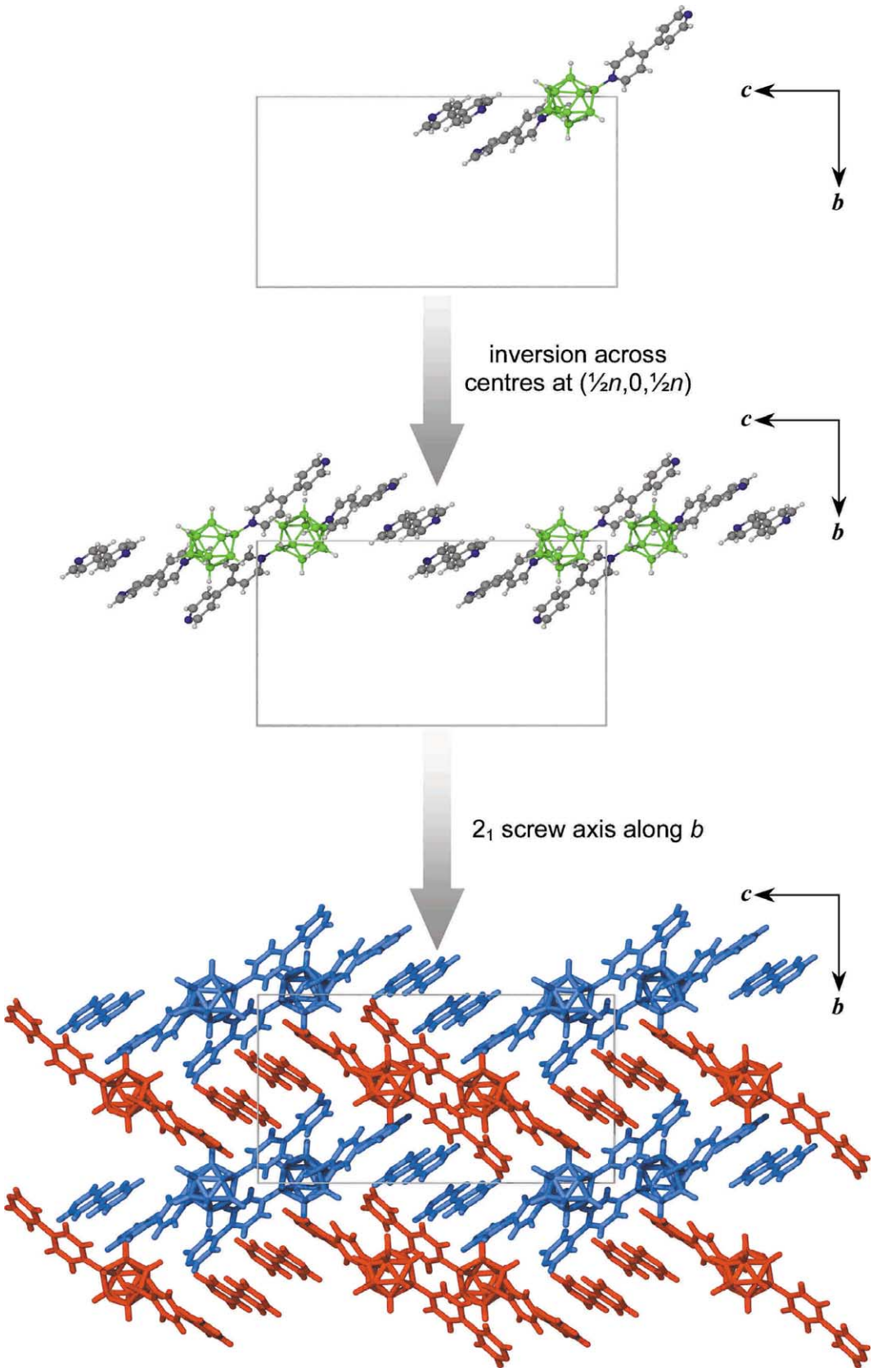

Fig. 3. The first two steps of KAP as applied to the 1:1 co-crystal of 4,4′-bipyridyl and [6,9-(4,4′-bipyridyl)$_2$-*arachno*-$B_{10}H_{12}$]. The pair of molecules closest to the unit cell origin (upper diagram) develop along successive inversion centres at ($\frac{1}{2}n$, 0, $\frac{1}{2}n$) to yield the inversion chain structure (centre diagram) and successive 2_1 screw axis operations along the crystallographic *b*-axis then generate the close-packed sheet (lower diagram). The chain components of sheet structure have been highlighted using alternate red and blue colours.

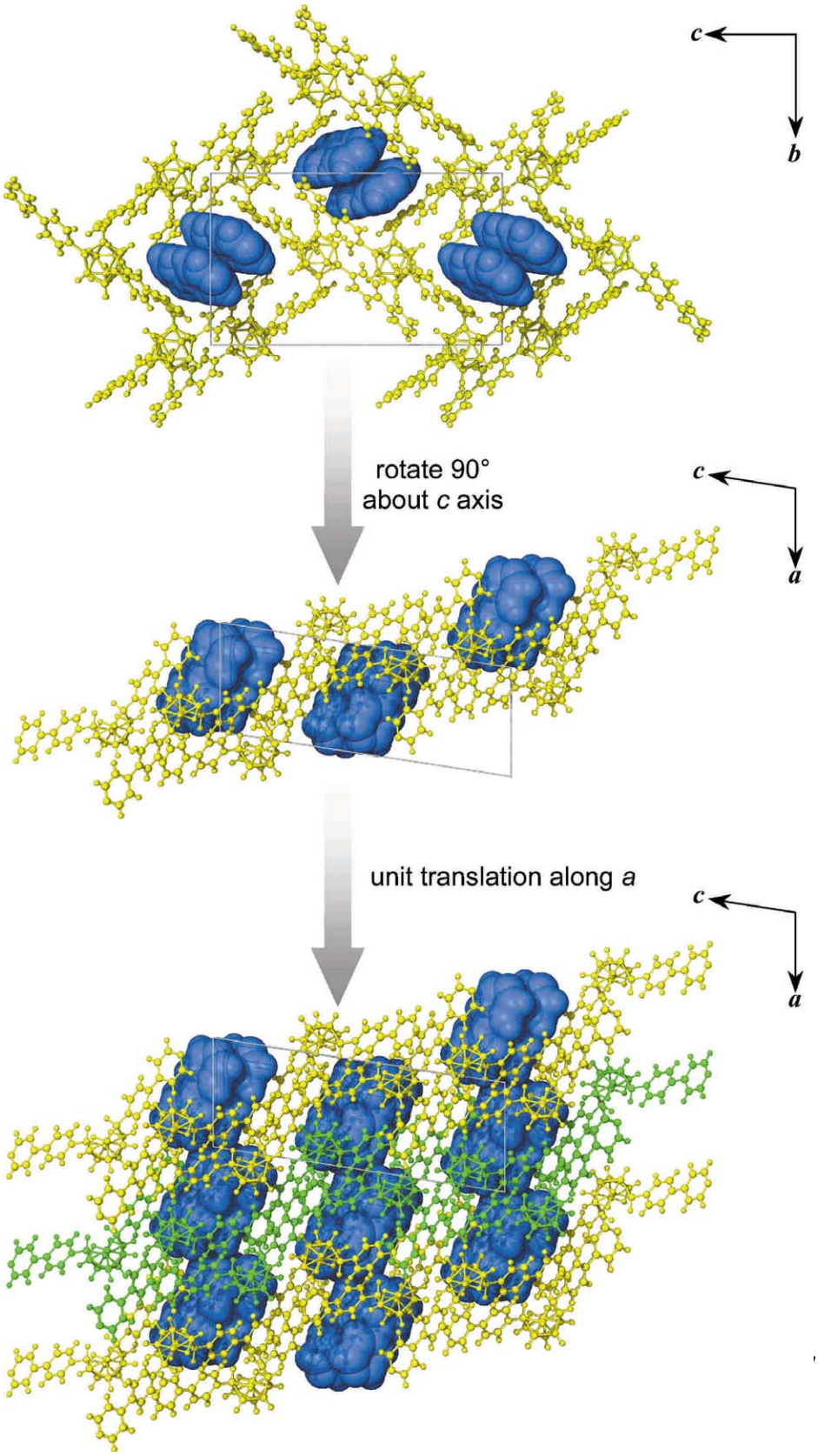

Fig. 4.

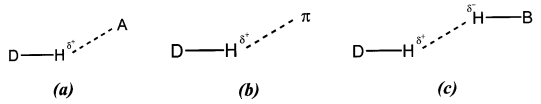

Fig. 5. Schematic representation of: (a) a classical hydrogen bond; (b) a non-classical hydrogen bond; and (c) a 'dihydrogen' bond.

esting supramolecular features, such as the incidence of channels and columns, may concomitantly be revealed and examined.

3.2. Dihydrogen-bonding and the crystal structure of H_3BNH_3

One of our developing interests is in the examination of weaker intermolecular attractive interactions involving borane species. One such interaction that is becoming increasingly recognised as important in structural borane chemistry is the so-called dihydrogen bond.

It is pertinent to summarise relevant aspects of dihydrogen-bonding and related phenomena [19–22]. A dihydrogen bond can be considered as having two components. These are generally described as 'donor' and 'acceptor' units (Fig. 5a). Confusion can arise here, however, because 'donor' and 'acceptor' are used in this dihydrogen-bonding context to describe hydrogen donors and acceptors [1], and thence have an opposite polar sense to the more commonly encountered concepts of Lewis-base donors and Lewis-acid acceptors. In the hydrogen-donor units considered here, hydrogen is bonded to a more electronegative element, so that the hydrogen atom is positively polarised. In a conventional hydrogen bond, this would then interact with the lone pair of an electronegative element, i.e. it would donate its positively polarised hydrogen atom to the negatively polarised electronegative element. In dihydrogen-bonding (Fig. 5c), the hydrogen-acceptor unit has its hydrogen atom bonded to a more electropositive element, such as, in the present context, boron. This negatively polarised hydrogen atom is regarded as accepting the positively charged hydrogen atom of the donor unit to form the dihydrogen bond. A positively polarised hydrogen atom can therefore interact attractively with a lone pair to form a conventional hydrogen bond, or with a negatively polarised hydrogen atom, e.g. that of a BH_3 group, to form a dihydrogen bond. Related to this, a positively polarised hydrogen atom can interact with an electron-rich π-system to form a weakly attractive π-to-hydrogen non-covalent bond (Fig. 5b). This last can also be significant in supramolecular assemblies of boron-containing cluster compounds. Of these 'weaker' interactions, the BH···HN dihydrogen-bonding interaction is the best examined in reported boron chemistry [19–22]. This bonding is typified by close interhydrogen approaches well within van der Waals radius sums, with interhydrogen distances well below 2.0 Å being common. There are also specific directional characteristics, with the BHH and NHH angles generally falling into the more acute and more obtuse ranges of 95–115 and 150–170°, respectively.

In borane chemistry, the classic example of dihydrogen-bonding is in 'ammonia borane', H_3BNH_3. This compound illustrates the dramatic effect of dihydrogen-bonding on physical properties, just like conventional hydrogen-bonding in, for example, with HF and H_2O. The H_3BNH_3 molecule is isoelectronic and isostructural, in gas-phase molecular terms, with the ethane molecule, H_3CCCH_3. However, H_3CCCH_3 melts at −181 °C, whereas H_3BNH_3 melts nearly 300° higher, at + 104 °C. Although some of this difference arises from the dipole moment of ammonia borane and consequent dipole–dipole attraction, this is probably not a significant contribution. Isoelectronic H_3CF, for example, which is a more polar molecule than H_3BNH_3, melts at −142 °C. It is currently thought that this higher melting point of H_3BNH_3 arises largely from dihydrogen-bonding [20].

The solid-state structure of H_3BNH_3 was reported some time ago (Fig. 6, top right) [19]. An analysis of the intermolecular close approaches in the crystalline lattice shows that in an individual H_3BNH_3 molecule, every hydrogen atom is involved in dihydrogen-bonding (Fig. 6, top left). Interestingly these are all bifurcated bonds; i.e. one NH donor unit is within dihydrogen-bonding distance of two acceptor BH units. Here we apply the KAP method to the appreciation of the overall dihydrogen-bonding network.

The compound crystallises in space group $Pmn2_1$. Each H_3BNH_3 molecule possesses crystallographic mirror symmetry. One H_3BNH_3 molecule can be placed near the origin (Fig. 6, centre right), and a 2_1 screw chain can thence be developed along the *c*-axis (Fig. 6, centre left). The series of dihydrogen bonds linking successive molecules is readily apparent. This chain substructure can then be developed into a sheet substructure by a permitted translation along the crystallographic *a*-axis (Fig. 6, lower). This reveals another set of dihydrogen bonds, now holding the chains together in a sheet. Here it may be pointed out that, conversely, and starting from the original molecule, an initial development of an *n*-glide chain along the [101] direction rather

Fig. 4. Blues Van der Waals representations highlight the local environments of pairs of 4,4′-bipyridyl co-crystal molecules in the sheet structure of the 1:1 co-crystal of 4,4′-bipyridyl and [6,9-4,4′-bipyridyl$_{12}$-*arachno*-$B_{10}H_{12}$] (upper diagram). The three-dimensional columnar architecture of the co-crystallite molecules is first illustrated by viewing down the *b*-axis along the *bc* plane (centre diagram) and generating the full three-dimensional structure by applying unit translations along the *a*-axis. Note that the sheet substructures have been highlighted using alternate yellow and green colours.

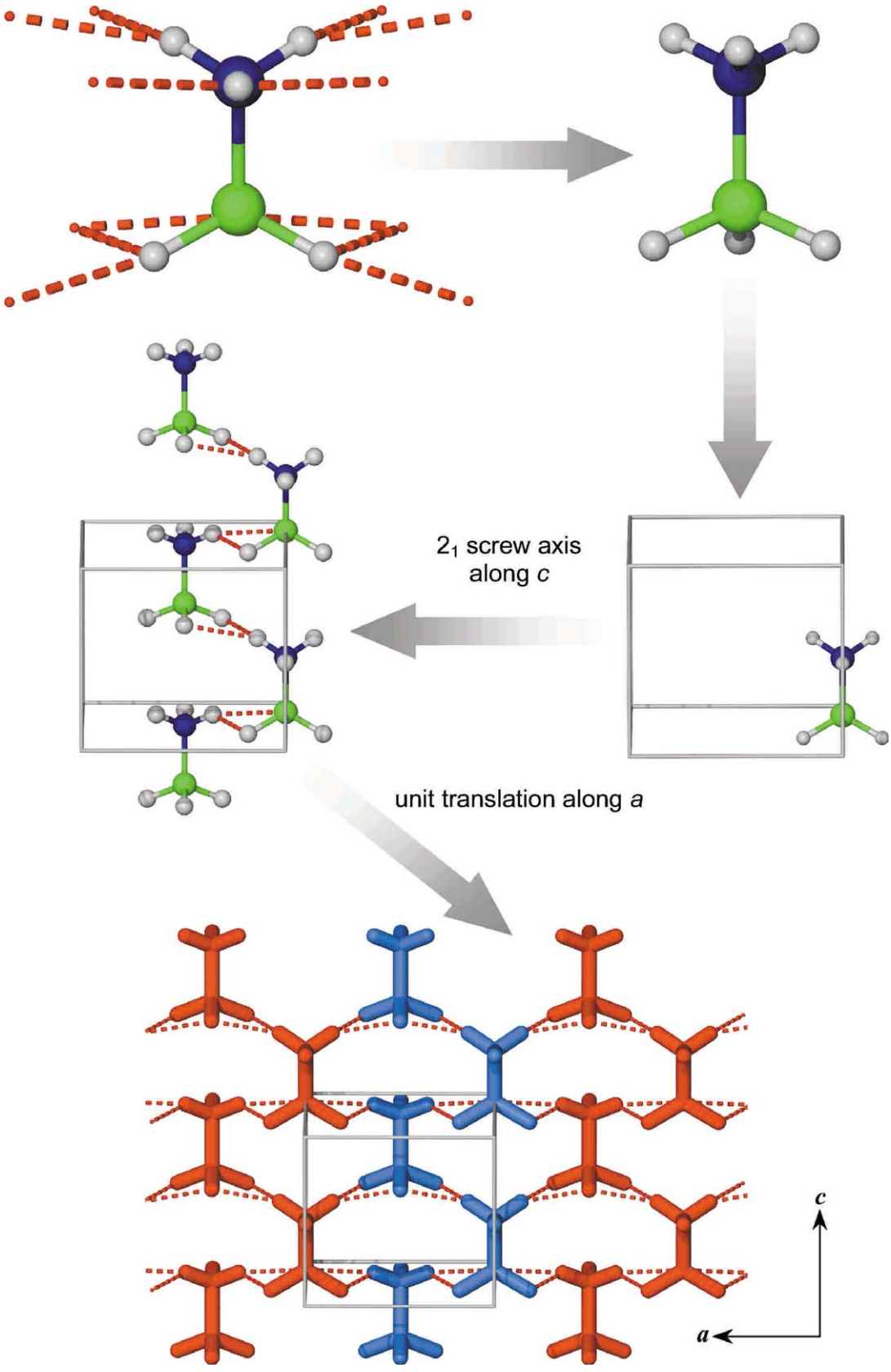

Fig. 6. The molecular structure of 'ammonia borane', H_3NBH_3, with intermolecular dihydrogen bonds included (top left), and omitted (top right), and the first two stages of KAP using a similar procedure to that illustrated in Fig. 3. The 2_1 screw axis along c at $a = \frac{1}{4}$, $b = 0$ is used to develop the chain structure (centre left) and successive unit translations along the crystallographic a-axis thence generate the close-packed sheet (lower diagram). The colour scheme follows the one used in Fig. 3.

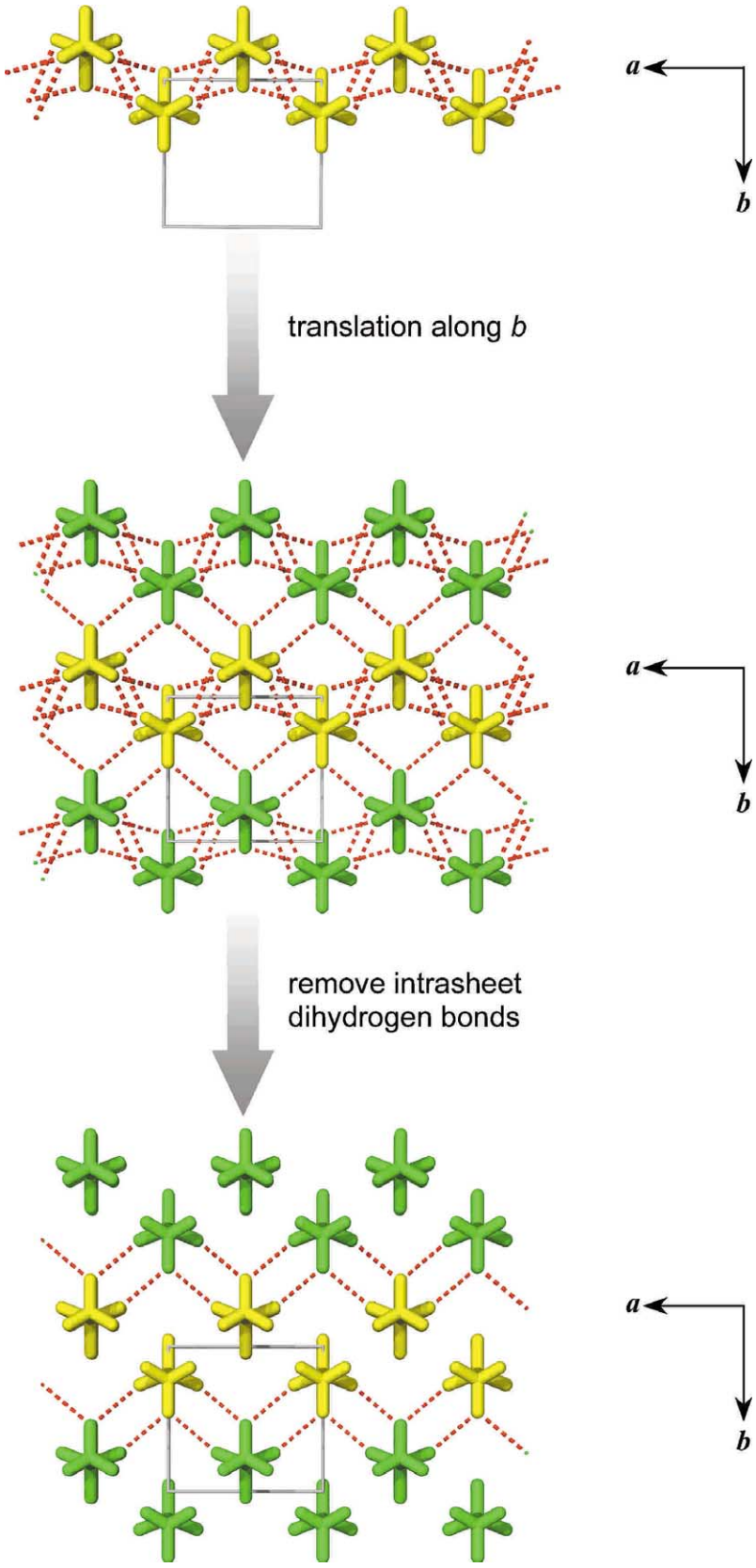

Fig. 7. The sheet substructure generated in Fig. 6, rotated by 90° about the *a*-axis (upper diagram), develops into the full three-dimensional structure by applying successive unit translations along the crystallographic *b*-axis. The resultant three-dimensional network appears complicated (centre diagram) but is considerably simplified when previously rationalised contacts within the sheet (Fig. 5) are omitted (lower diagram). The colour scheme follows the one used in Fig. 4.

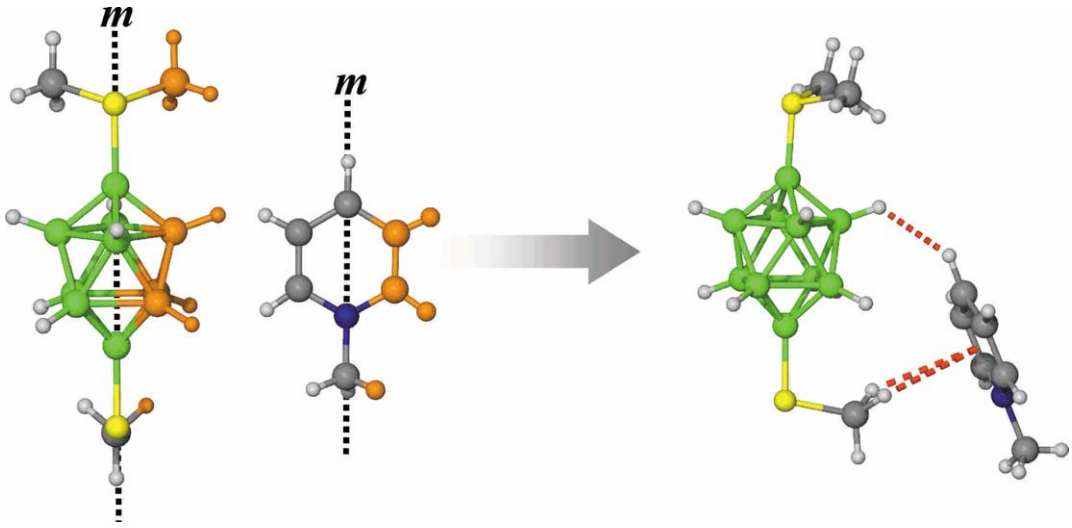

Fig. 8. The molecular structure of the salt $[C_5H_5NMe]^+[1\text{-}(SMe)\text{-}10\text{-}(SMe_2)\text{-}closo\text{-}B_{10}H_8]^-$, viewed as individual components (left) and as a closely interacting ion-pair (right). Both components possess crystallographic C_s symmetry and symmetry-generated parts of the ions are highlighted in orange in the left-hand diagram.

than the screw chain along the *c*-axis, followed by successive unit translations along the *a*-axis, would also generate the same two-dimensional sheet. One corollary here is that there is inherent capability in the KAP method to choose among chain-generation steps to single out particular intermolecular features; this provision is generally applicable.

The generation of the macroscopic crystal structure of H_3BNH_3 from this KAP sheet is conveniently envisaged via the orthogonal view in the *bc* plane, looking along the crystallographic *b*-axis (Fig. 7, upper diagram). The sheet structure develops into the macro structure via successive unit translations along the crystallographic *b*-axis (Fig. 7, centre). This develops the entire network of dihydrogen bonds that binds the crystal together so effectively. The individual interactions constitute a complex matrix that is difficult to elucidate in diagrams such as this. However, the removal from the diagram of all the dihydrogen bonds associated with the development of the initial chain and sheet substructure readily distinguishes the intersheet dihydrogen bonds (Fig. 7, lower). The KAP methodology therefore nicely enables a clearer analysis and understanding of what at first appears to be a very complicated three-dimensional network of interactions (Fig. 6, upper left). It therefore can give an improved analysis and appreciation beyond that originally presented [19,20].

3.3. Solvent channels and the structure of the co-crystal of *n*-hexane with the $[C_5H_5NMe]^+[1\text{-}(SMe)\text{-}10\text{-}(SMe_2)\text{-}closo\text{-}B_{10}H_8]^-$ salt

The KAP discernment of channels within the crystal lattice is illustrated using Example 1 above, the 1:1 co-crystal of 4,4′-bipyridyl and $[6,9\text{-}(4,4'\text{-bipyridyl})_2\text{-}arachno\text{-}B_{10}H_{12}]$. Here, the approach is developed to define the nature of an interesting channel structure in the $[C_5H_5NMe]^+$ salt of the $[1\text{-}(SMe)\text{-}10\text{-}(SMe_2)\text{-}closo\text{-}B_{10}H_8]^-$ anion (CCDC deposition no. 172366). A channel structure that supported by a network of weak hydrogen- and dihydrogen-bonding is revealed. Interestingly, the channels are filled by *n*-hexane solvent of crystallisation.

The salt can be synthesised by the heating of the ten-vertex neutral species $[1,10\text{-}(SMe_2)_2\text{-}closo\text{-}B_{10}H_8]$ with refluxing pyridine [12]. This reaction has precedent, for example in the demethylation of the twelve-vertex analogue $[1,12\text{-}(SMe_2)_2\text{-}closo\text{-}B_{12}H_{10}]$ to give the $[1\text{-}(SMe)\text{-}12\text{-}(SMe_2)\text{-}closo\text{-}B_{12}H_{10}]^-$ anion [23]. The $[1\text{-}(SMe)\text{-}10\text{-}(SMe_2)\text{-}closo\text{-}B_{10}H_8]^-$ anion itself is of straightforward ten-vertex *closo* cluster constitution (Fig. 8, left), and *N*-alkylpyridinium cations $[C_5H_5NR]^+$ are, of course, well recognised. The compound itself is therefore not unusual in terms of its molecular components. However, even the preliminary step of the KAP approach reveals an interesting close interionic interaction (Fig. 8, right).

Thus, there is a close CH···HB intermolecular approach of 2.11 Å.[3] The interaction involves the *para*-CH unit of the cation and the BH unit in the 4-position of the cluster anion (Fig. 8, right). In the general case, a CH···HB dihydrogen-bonding interac-

[3] Distances and angles throughout this text are derived using were calculated using 'normalised' hydrogen atom positions [31]. These positions are based on neutron-diffraction measurements [1] and are used because they minimise the systematic errors associated with the location of hydrogen-atom centres in structures determined by X-ray diffraction analysis, and enable comparisons to be made between structures on a consistent basis [32].

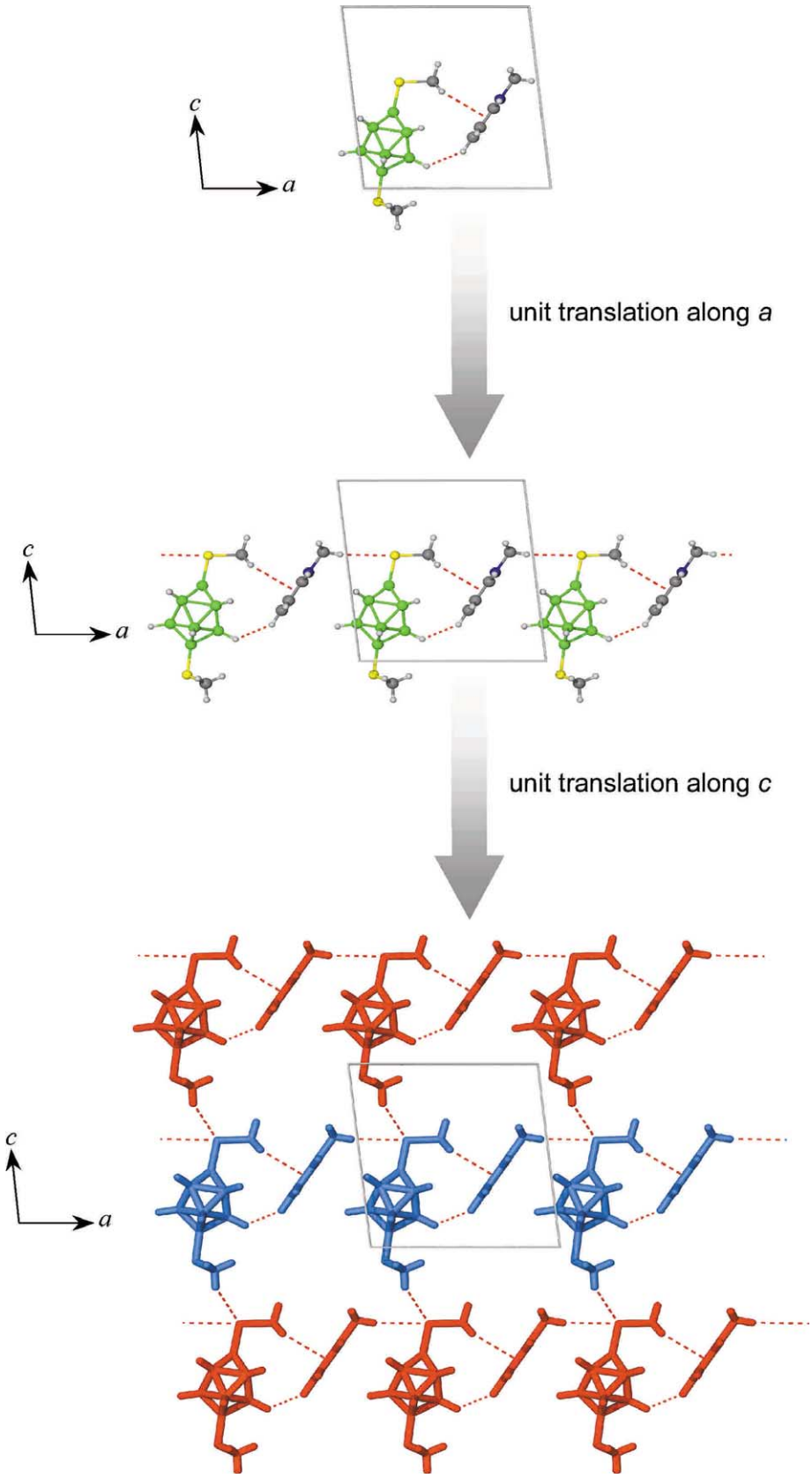

Fig. 9. The first two steps of the KAP method as applied to $[C_5H_5NMe]^+[1\text{-}(SMe)\text{-}10\text{-}(SMe_2)\text{-}closo\text{-}B_{10}H_8]^-$. A procedure similar to that illustrated in Fig. 3 is adopted, using successive unit translations to develop the chain structure (centre diagram) and the close-packed sheet (lower diagram) along the crystallographic *a*- and *c*-axes, respectively. The colour scheme follows that used in Fig. 3 with intermolecular close contacts shown as hatched red lines.

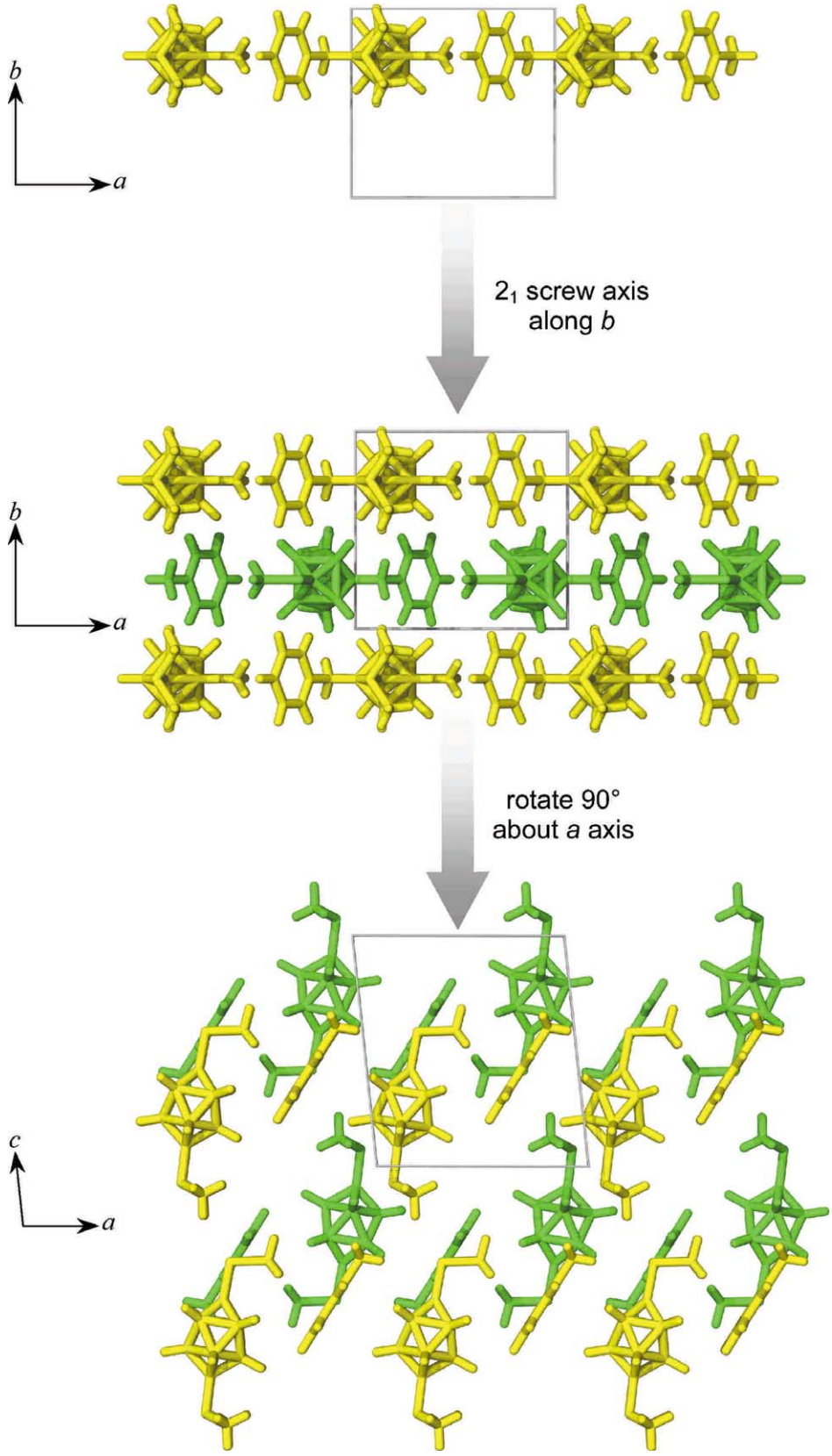

Fig. 10. The sheet structure of $[C_5H_5NMe]^+[1\text{-}(SMe)\text{-}10\text{-}(SMe_2)\text{-}closo\text{-}B_{10}H_8]^-$ of Fig. 9, viewed down the crystallographic *c*-axis along the *ac* plane (upper diagram), develops into the full three-dimensional structure when successive 2_1 screw axis operations are applied along the crystallographic *b*-axis (centre diagram). The relatively flat sheets do not interpenetrate and the void spaces apparent in the sheet structure of Fig. 9 thus develop into sets of parallel channels (lower diagram). The colour scheme used follows that used in Fig. 4.

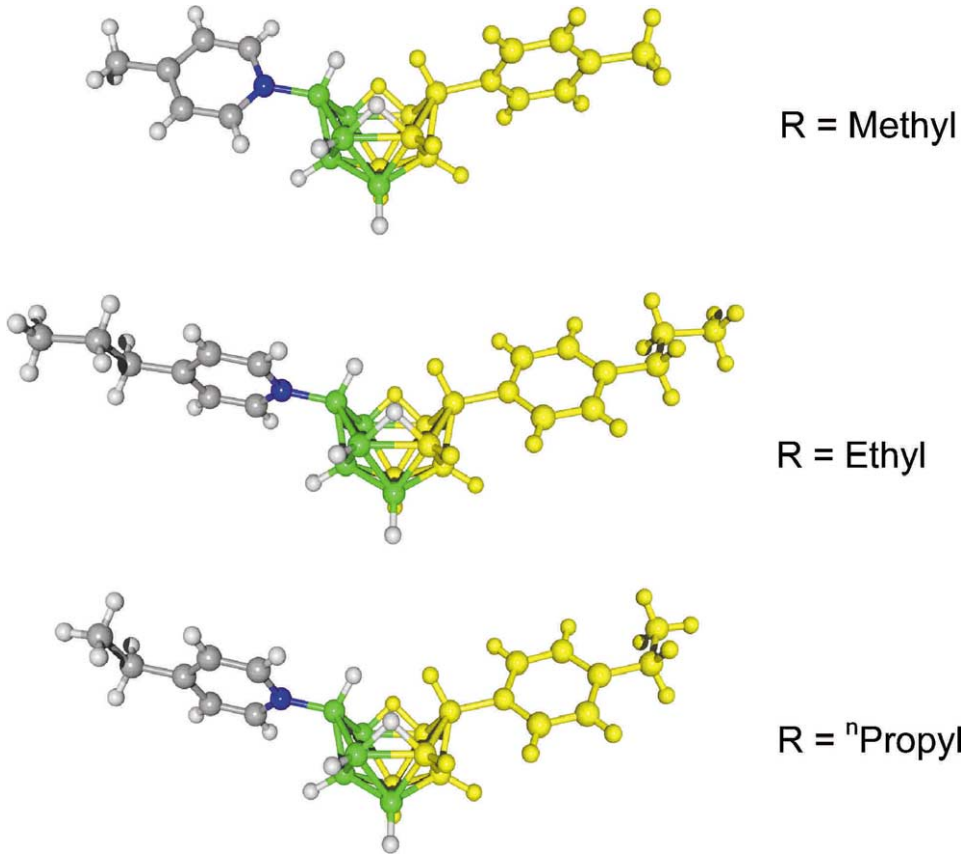

Fig. 11. The molecular structures of [6,9-(NC_5H_4–4-R)$_2$-*arachno*-$B_{10}H_{12}$], where R is Me (upper), Et (middle) and *n*-Pr (lower). All three structures possess crystallographic C_2 symmetry and symmetry-generated parts of each molecule are coloured yellow.

tion tends to be weaker than NH···HB because of the lower polarisation of the CH unit compared to NH. Here, however, the attraction is enhanced somewhat because of the anion–cation polarity inherent in this ionic species. It can also be seen that there is a close interionic CH···π approach [24]. This CH···π combines with the CH···HB interionic attraction to bind the ion-pair unit together. This $[C_5H_5NMe]^+$[1-(SMe)-10-(SMe_2)-*closo*-$B_{10}H_8]^-$ ion-pair unit can be positioned near the origin (Fig. 9, upper). The space group is $P2_1/m$ and a KAP chain structure can be generated by a translational operation along the crystallographic *a*-axis (Fig. 9, centre). This translational operation reveals close CH···S approaches [25] between the ion-pair in the developed chain substructure. As with the CH···HB and CH···π attractions just mentioned, this (more conventional) CH···S hydrogen-bonding will be weak [25], but here will be enhanced somewhat by the S acceptor being associated with the anion, and the positively polarised CH hydrogen donor associated with the cation.

The next KAP step, sheet generation, is accomplished by another straightforward translation, now along the crystallographic *c* axis (Fig. 9, lower). A second set of weak CH···S interactions now becomes apparent and, overall, the sheet substructure can be described as ion-pair units held together by a two-dimensional network of CH···HB dihydrogen bonds and CH···S hydrogen bonds. Examination of the two-dimensional sheet reveals significant intermolecular voids and it is necessary to establish whether these are true voids in the three-dimensional overall structure, and, if so, whether they are they defined pockets. Alternatively, the voids may develop into continuous channels in the three-dimensional lattice when the third symmetry operation is applied. A third possibility is that some protuberance from the two-dimensional sheet may fill the void in the adjacent sheet so that no pockets or channels prevail.

The side-view of this two-dimensional sheet along the *c* direction in the *ac* plane demonstrates a relatively flat configuration (Fig. 10, upper). Consequently, there is no significant protuberance from one sheet into an adjacent sheet when successive 2_1-screw operations are applied along the crystallographic *b*-axis to generate the observed overall three-dimensional lattice in the final KAP step (Fig. 10, centre). The orthogonal view down the crystallographic *b*-axis (Fig. 10, lower) thence shows that the voids in one layer (coloured yellow) are positioned directly above voids in the adjacent layer (coloured green). The voids thus develop into a series of parallel channels passing through the crystal in the

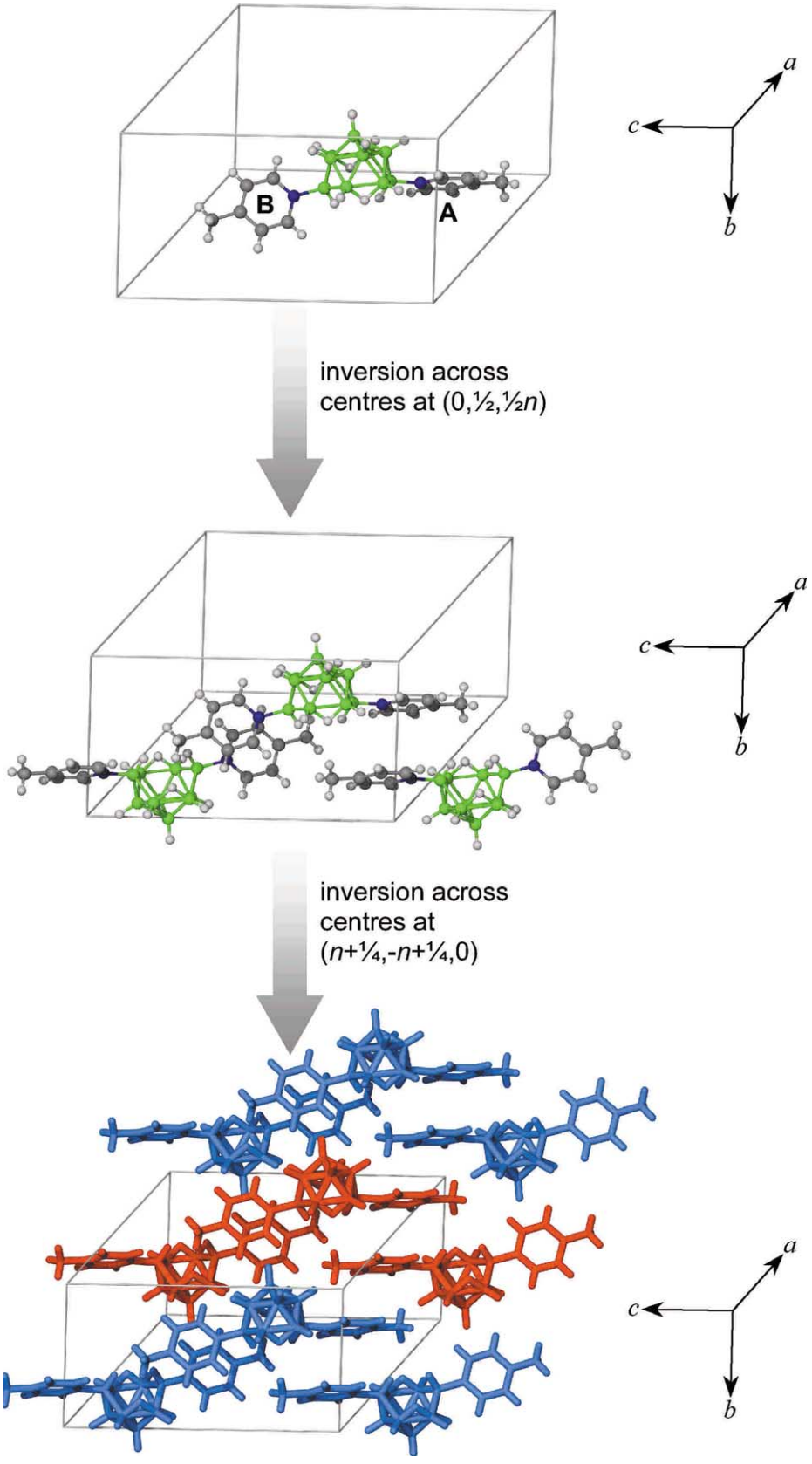

Fig. 12. The first two steps of the KAP method as applied to [6,9-$(NC_5H_4$–4-Me$)_2$-*arachno*-$B_{10}H_{12}$]. The procedure used follows that illustrated in Fig. 3, but with inversion centres used to generate both the chain and sheet structures, which are illustrated in the centre and lower diagrams, respectively. The colour scheme is the same as the one used in Fig. 3.

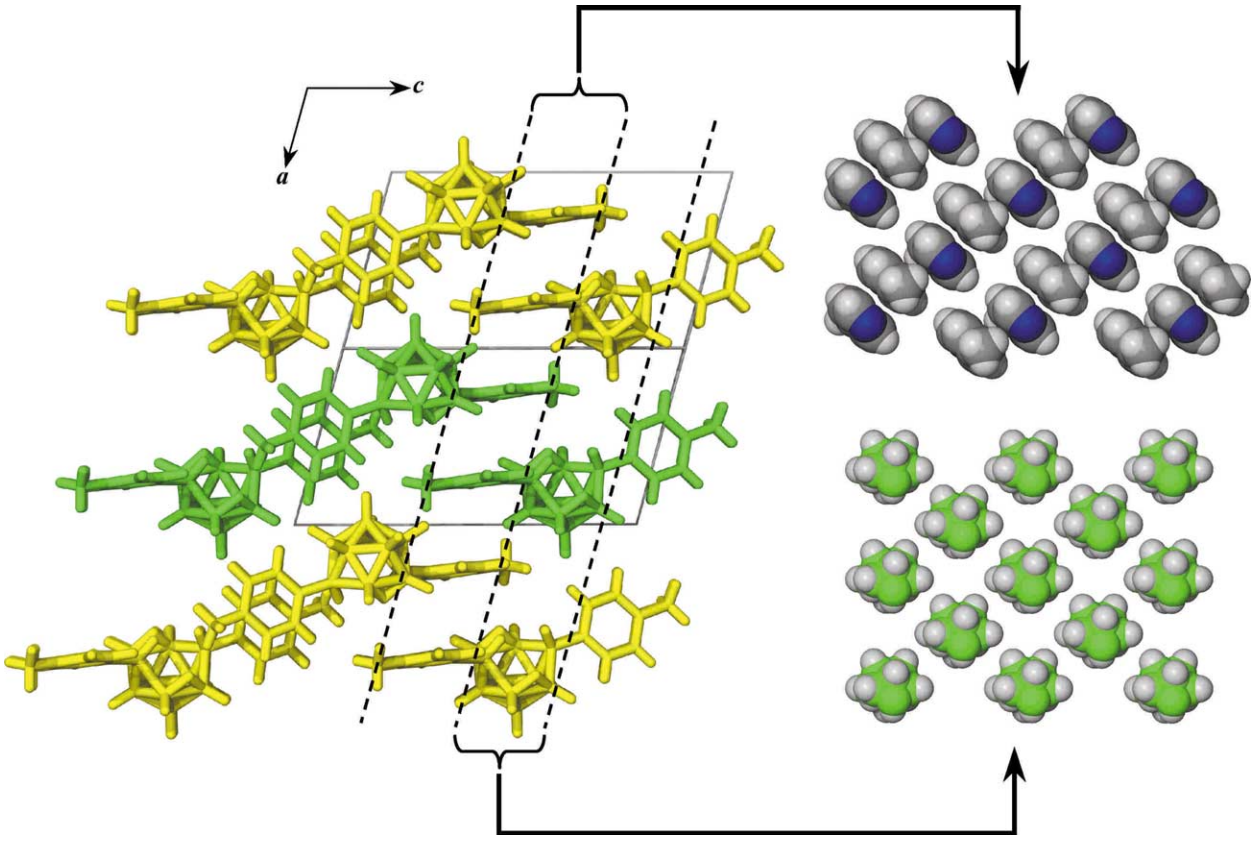

Fig. 13. The three-dimensional structure of [6,9-(NC_5H_4–4-Me)$_2$-*arachno*-$B_{10}H_{12}$] (left) obtained at the third KAP step by applying successive unit translations, along the crystallographic *a*-axis, to the sheet structure of Fig. 12. The structure is viewed down the crystallographic *b*-axis, in the plane of the sheet structures. The alternate sheet components are highlighted using alternate yellow and green colours. The three-dimensional structure can be envisaged in terms of alternating layers in the *ab* plane of pyridine units (upper right) and borane cages (lower right).

crystallographic *b*-direction. Examination of these channels reveals that they are internally lined with hydrogen atoms (Fig. 10, lower). These hydrogen atoms are held in close proximity to one another by weak intermolecular attractive interactions, either by dihydrogen-bonding [19,20], or by the unusual CH···S interactions mentioned above. Interestingly, the channels are occupied by linear *n*-hexane molecules, derived from the solvent of crystallisation, the crystal having been grown by diffusion of *n*-hexane into a solution of the compound in CH_2Cl_2 at room temperature. The hexane molecules are disordered, perhaps because there is insufficient differentiation of polarisability among the hydrogen atoms that line the tubular cavity to attract the hexane molecule particularly to one part of the cavity rather than another. The recognition of the channel structure may not have arisen in the absence of the KAP three-dimensional analysis.

An interesting speculation arises from the recognition of such channels. If they could be constructed to be framed with molecules that held reactive groups that might then readily partake covalent intermolecular cross-linking, then the possibility exists that the mild curing of such molecular crystalline solids could induce precursors for solid-state ceramic materials with tailored mesoporic channels and cavities. This would imply very specific crystal engineering, for which it would be necessary to tailor and tune the crystal structure very finely. In order to do this, more knowledge of the interplay of the intermolecular binding factors would be required than is presently available. Initial steps along this pathway can, however, be made by the systematic examination of how a given intermolecular structural paradigm systematically varies among a closely related series of compounds, as exemplified in Example 4 below.

4. Systematic variations within the crystal structures of [6,9-(NC_5H_4-4-R)$_2$–*arachno*-$B_{10}H_{12}$], where R is Me, Et and *n*-Pr

The bis(pyridine) *arachno* decaboranes [6,9-(NC_5H_4R)$_2$-*arachno*-$B_{10}H_{12}$] can be readily made from the displacement by the pyridines of the weaker donor SMe_2 from the bis(dimethylsulphide) analogue [6,9-(SMe_2)$_2$-*arachno*-$B_{10}H_{12}$] [14,18,26]. The last compound is readily made quantitatively from the commonly used starting material $B_{10}H_{14}$ by a simple heating in SMe_2

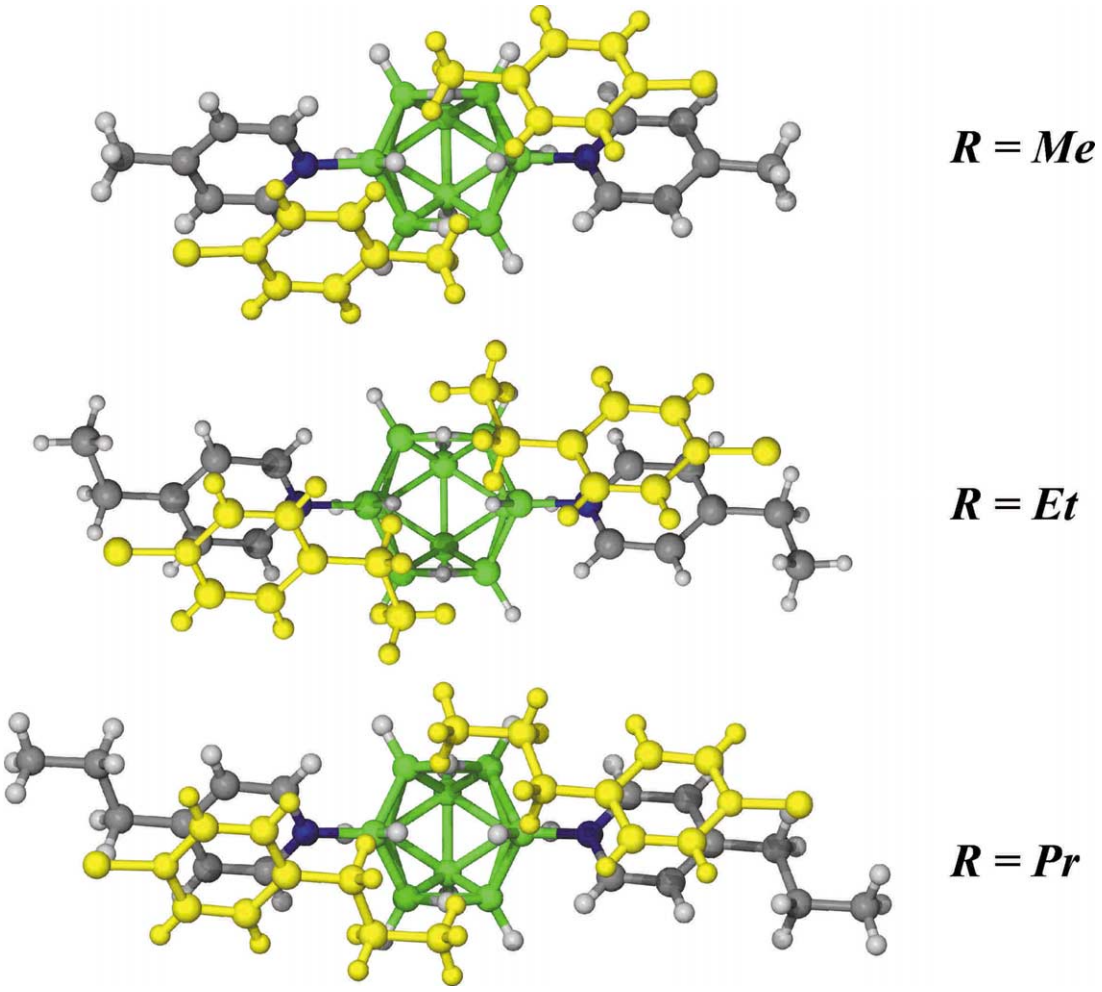

Fig. 14. The relative positioning of a pair of symmetry-related alkyl pyridine units over the open face of a borane cluster in the second-step KAP chains of [6,9-(NC_5H_4–4-R)$_2$-*arachno*-$B_{10}H_{12}$], where R is Me (upper), Et (middle) and *n*-Pr (lower). The symmetry-related pyridine units are highlighted in yellow.

solution [27,28]. Since whole varieties of substituted pyridines are readily available, several related series of compounds can readily be made for the systematic examination of the variations of intermolecular behaviour within their crystals. The short series of *para*-alkylated pyridine derivatives [6,9-(NC_5H_4–4-R)$_2$-*arachno*-$B_{10}H_{12}$], where R is systematically longer along the progression methyl, ethyl and *n*-propyl is used here to as an illustrative example (Fig. 11).

The *para*-methyl derivative [6,9-(4-Me–C_5H_4N)$_2$-*arachno*-$B_{10}H_{12}$] crystallises in space group *C*2/*c* (CCDC deposition no. 172368). As for the examples above, the molecule is most conveniently positioned as close to a unit-cell origin as possible, (Fig. 12). It can be seen that both the 6- and 9-positioned pyridine ring systems are quite close to inversion centres, at (0, $\frac{1}{2}$, 0) and (0, $\frac{1}{2}$, $\frac{1}{2}$), respectively, marked as A and B in the diagram (Fig. 12, upper). The propagation of the molecules across these inversion centres generates an inversion chain parallel to the crystallographic *c*-axis, (Fig. 12, centre). It can be seen that these successive inversion operations generate pairs, or 'diads', of aromatic rings in close contact. A second set of inversion operations constitutes the second KAP step. The inversion centres are at ($n+\frac{1}{4}$, $-n+\frac{1}{4}$, 0), where $n = 0, \frac{1}{2}, 1, 1\frac{1}{2}, 2, \ldots$ The original inversion chain thereby develops into a two-dimensional sheet substructure in the [1, 1, 0] plane (Fig. 12, lower). In the Figure, successive chains are coloured differently to clarify the structural evolution. In this last view, which is perpendicular to the sheet substructure, it can be seen that one of ring diads of the chain, marked A, aligns with the corresponding diads in successively adjacent chains to develop into an extended stack of aromatic rings. The other diad, marked B, remains ostensibly isolated, but the orthogonal view along the [1, 1, 0] plane (Fig. 13, left), followed by unit translations of the sheet structure along the crystallographic *a*-direction in the last KAP step to generate the complete lattice, shows that these B diads also develop into an extended ring stack. There are

thus two orthogonal ring-stacks, one in the [1, 1, 0] direction, and one in the [−1, 1, 0] direction.

At this stage, it is interesting to note that alternative sections through the lattice can effectively isolate sheets of pyridine rings and sheets of boron cages. Thus, if a section is taken in an *ab*-plane through one of the ring stacks in (Fig. 13, left), then a sheet of pyridine rings, comprised of mutually adjacent ring-stacks, is revealed (Fig. 13, upper right). Similarly, a parallel sheet of borane cages is revealed in the *ab*-plane when a corresponding section is taken through an adjacent set of borane cages (Fig. 13, lower right). The crystal structure may therefore be envisaged in terms of alternating sheets of pyridine rings and sheets of boron cages. It can be seen that there is a quasi-hexagonal arrangement of each of these sets of rings and cages in their respective sheets, consistent with and nicely illustrating the close-packing principles behind the KAP approach.

It can also be of interest to speculate on the possibility of cross-linking such sheets of carbon-containing rings and boron-containing clusters. If such a cross-linking were followed by a thermal curing to eliminate hydrogen, then ultimately ceramic boron–carbon–nitrogen materials layered at the atomic dimension could be engendered. These bis(pyridine)-*arachno*-decaborane species are, however, prone to disproportionation under heating to give pyridinium salts of the [*closo*-$B_{10}H_{10}]^{2-}$ anion (Eq. (1)). The stoichiometric and quantitative thermolysis of the $B_{10}H_{12}L_2$ bis(amine) decaboranes to give the corresponding ammonium salts of the *closo*-$[B_{10}H_{10}]^{2-}$ anion has been known for over 40 years, and constitutes a standard preparative route to this anion [29]. In the pyridinium salts, this reaction disrupts the lattice, ultimately giving an amorphous ceramic material [30]. Prevention of the disproportionation could possibility be achieved by tailoring the lattice structure to engender very close CH···HB or NH···HB contacts which may then be prone to dihydrogen elimination under very mild curing conditions to develop C–B or N–B cross-linked layer structures at the pre-ceramic stage. As with the possibilities for channel-structured materials discussed in Example 3 above, this implies very specific crystal engineering involving very fine-tuning of the structure: more knowledge of the subtle interplay of the intermolecular binding factors would be required than is presently available.

$$[(MeC_6H_4)_2B_{10}H_{12}] \rightarrow 2[MeC_5H_4NMe]^+ + [B_{10}H_{10}]^2 \quad (1)$$

One component of this approach would be a recognition of factors influencing the relative intermolecular positioning of intramolecular components. In this regard, a careful yet consistently systematic comparison of the 4-methyl pyridine compound above with its 4-ethyl and 4-*n*-propyl analogues illustrates how this may be approached. Specifically, the effect of a successive increase in chain length of the *para*-alkyl group on the pyridine unit is examined. The two additional compounds [6,9-(NC_5H_4–4-Et)$_2$-*arachno*-$B_{10}H_{12}$] (CCDC deposition no 172369) and [6,9-(NC_5H_4–4-*n*-Pr)$_2$-*arachno*-$B_{10}H_{12}$] (CCDC deposition no 172370), both also crystallise in space group *C*2/*c*. Generating first the chain structure, then the sheet structure, and then the macromolecular structure, each can be developed in the same way as for the methyl species (Figs. 12 and 13).

The three successive KAP operations, giving an inversion chain, an inversion generated sheet, and finally a translation to generate the observed lattice, are very similar for all three, although in the latter two cases different inversion centres are applied as appropriate. Fig. 14 compares features of the KAP step-1 chain structure for the three compounds, and the similarities are clear. Thus, corresponding ring-diads are clearly apparent in all three chains, and it can be seen in each case that there are two alkyl groups positioned above the open face of the boron cage. It can also be seen that, as this alkyl group gets larger, from methyl to ethyl, the two symmetry-related alkyl groups from nearest-neighbour molecules in the chain start increasingly to avoid each other by wrapping around, but remaining over, the open face of the cage. The effect is continued for the longer *n*-propyl residue, which almost embraces the open face completely. The concomitant effect, as the progressively longer alkyl group has to be accommodated over the open face, is to shift the two pyridine rings in the diads over one another, with the result that the chain progressively expands along the chain axis. The carbon atom in the 4-position on the pyridine unit can be conveniently used as an indicator for this shift. In the methyl compound this carbon atom is seen to be directly above the boron atom in the 'prow' position of the boron cage of the adjacent molecule (Fig. 14, upper diagram). In the ethyl compound this atom is shifted away from the open face of the boron cluster so that now it approaches the nitrogen atom of the pyridine ring underneath it (Fig. 14, centre). In the *n*-propyl compound this atom has progressed still further, and is now positioned on the far side of the nitrogen atom of the pyridine ring (Fig. 14, lower). Therefore, as the length of the alkyl chain increases, the basic chain structure is not destroyed. Rather, an effective slippage of the basic structure along the chain direction occurs to accommodate the increased alkyl chain length. This analysis therefore nicely illustrates the subtle effects on the supramolecular lattice that can arise from the variation of but one molecular parameter. The effects these and other parameters on the 'fine-tuning' of crystal structure of boron-containing species is the subject of continuing current research in our laboratories.

5. Conclusion

KAP constitutes a most useful method for the systematic analysis of molecular packing arrangements that compliments and extends other approaches. The KAP approach simplifies the visualisation of molecular packing by breaking it down into a series of symmetry-generated steps. Each step permits all intramolecular interactions, even the weakest, in that particular step to be readily identified. Thence, cumulatively, as the steps build up to generate the observed three-dimensional crystal lattice of molecules, an understandable view of the complex three-dimensional molecular interaction network is readily and systematically built up. For example, within the polyhedral boron-containing cluster systems illustratively examined here, KAP has enabled: (a) a rigorous approach to the identification and study of molecular encapsulation effects; (b) the identification and rationalisation of the NH···HB dihydrogen-bonding network of BH_3NH_3; (c) the analysis of the bonding involved in the architecture of solvent-occupied lipophilic channels in an ionic *closo* decaborane compound; and (d) the systematic identification and examination of subtle trends in supramolecular aggregation in closely related molecules which may have significant implications in developing the field of crystal engineering. It is to be emphasised that the examples chosen are to illustrate the method. The small number does not encompass the full range of solid-state phenomena to be identified and subsequently analysed using KAP. The extension to the full range of phenomena in polyhedral boron-containing cluster systems, and to increasing complexities of combinations of phenomena augurs well for the discovery, delineation and development of much new and interesting boron-based supramolecular physics and chemistry.

6. Supplementary material

Crystallographic data for the structural analysis have been deposited with the Cambridge Crystallographic Data Centre, CCDC nos. 172365, 172366, 172368–172370 for compounds [6,9-(4,4′-bipy)$_2$-*arachno*-$B_{10}H_{12}$], [1-(SMe)-10-(SMe_2)-*closo*-$B_{10}H_8]^-$, [6,9-(4-Me–C_5H_4N)$_2$-*arachno*-$B_{10}H_{12}$], [6,9-(NC_5H_4–4-Et)$_2$-*arachno*-$B_{10}H_{12}$] and [6,9-(NC_5H_4-4-*n*-Pr)$_2$-*arachno*-$B_{10}H_{12}$], respectively. Copies of this information may be obtained free of charge from The Director, CCDC, 12 Union Road, Cambridge CB2 1EZ, UK (Fax: +44-1223-336033; e-mail: deposit@ccdc.cam.ac.uk or www: http://www.ccdc.cam.ac.uk).

Acknowledgements

We thank L.B. (Columbia, Missouri) for specific adaptations to his XSeed program, Ton Spek (Utrecht) for specific additions to his PLATON program, and the EPSRC (grants nos. GR/L/49505 and GR/M/83360) for support and for a studentship to Caroline O'Dowd. We also thank M.L. and J.H. for the supply of crystalline compounds and for permission to use results before formal publication [12,13], and T.W. for technical collaboration in alternative methods of manuscript preparation derived from oral presentations.

References

[1] G.R. Desiraju, T. Steiner, The Weak Hydrogen Bond in Structural Chemistry and Biology, Oxford University Press, Oxford, England, 1999 pp. 1–21.
[2] See, for example: G.R. Desiraju, Crystal Engineering: The Design of Organic Solids, Elsevier, Amsterdam, 1989.
[3] M.C. Etter, Accs. Chem. Res. 23 (1990) 120 (and references cited therein).
[4] (a) J. Bernstein, M.C. Etter, J.M. MacDonald, J. Chem. Soc. Perkin Trans II (1990) 695;
(b) J. Bernstein, R.E. Davis, L. Shimoni, N.-L. Chang, Angew. Chem. Int. Ed. Engl. 34 (1995) 1555.
[5] A.I. Kitaigorodskii, Organic Chemical Crystallography, Consultants Bureau, New York, 1961.
[6] See, for example: A.R. West, Basic Solid State Chemistry, 2nd ed., Wiley, Chichester, England, 1999 pp. 21–30.
[7] F. Allen, O. Kennard, Chem. Design Automat. News 8 (1993) 31.
[8] J. Perlstein, in: D. Braga, F. Greponi, A.G. Orpen (Eds.), Crystal Engineering: From Molecules and Crystals to Materials, Kluwer Academic Press, Netherlands, 1999, p. 23.
[9] (a) J. Perlstein, K. Steppe, S. Vaday, E.M.N. Ndip, J. Am. Chem. Soc. 118 (1996) 8433;
(b) J. Perlstein, J. Amer. Chem. Soc. 116 (1994) 455;
(c) J. Perlstein, J. Am. Chem. Soc. 116 (1994) 11420;
(d) J. Perlstein, Chem. Mater. 6 (1994) 319;
(e) J. Perlstein, J. Am. Chem. Soc. 114 (1992) 1955.
[10] (a) C. Price, M. Thornton-Pett, J.D. Kennedy, Abstracts ERICE, Esperantino, Sicily, May 15–20 1999, Abstract no. A42;
(b) C. Price, M. Thornton-Pett, J.D. Kennedy, Abstracts Tenth International Meeting on Boron Chemistry (IMEBORON X), Durham, England, July 11–15 1999, Abstract no. PA-39, p. 143;
(c) C. Price, J.D. Kennedy, M. Thornton-Pett, Abstracts Third RSC Dalton Discussion—Inorganic Crystal Engineering, Bologna, Italy, 9–11 September 2000, Abstract no. 28;
(d) L.M. Brown, C. Price, J.D. Kennedy, M. Thornton-Pett, Abstracts Third RSC Dalton Discussion—Inorganic Crystal Engineering, Bologna, Italy, 9–11 September 2000, Abstract no. 29;
(e) C. O'Dowd, L.M. Brown, S.L. Shea, U. Dörfler, J.D. Kennedy, C.A. Kilner, M. Thornton-Pett, Abstracts Second European Symposium on Boron Chemistry, EUROBORON 2, Dinard, France, 2–6 September, 2001, Abstract no. O32.
[11] C. O'Dowd, J.D. Kennedy, S.L. Shea, T.M. Polyanskaya, V.E. Volkov, W. Clegg, S.J. Teat, M. Thornton-Pett, Crystal Growth and Design, to be submitted.
[12] J. Holub, C. O'Dowd, J.D. Kennedy, Mark Thornton-Pett, Crystal Growth and Design, to be submitted.
[13] M. Londesborough, C. O'Dowd, J.D. Kennedy, M. Thornton-Pett, Crystal Growth and Design, to be submitted.

[14] C. O'Dowd, Thesis, University of Leeds, 2001.
[15] A.V. Shubnikov, V.A. Koptsik, Symmetry in Science and Art, Plenum Press, New York, 1974, pp. 103–127.
[16] R.P. Scaringe, S. Perez, J. Phys. Chem. 91 (1987) 2394.
[17] R.P. Scaringe, in: J.R. Fryer, D.L. Dorset (Eds.), Electron Crystallography of Organic Molecules, Kluwer Academic Press, Netherlands, 1990, p. 85.
[18] S.G. Shore, in: E.L. Meutterties (Ed.), Boron Hydride Chemistry, Academic Press, New York, 1975, pp. 79–174.
[19] W.T. Klooster, T.F. Koetxle, P.E.M. Seigbahn, T.B. Richardson, R.H. Crabtree, J. Am. Chem. Soc. 121 (1999) 6337.
[20] T.B. Richardson, S. de Gala, R.H. Crabtree, J. Am. Chem. Soc. 117 (1995) 12875.
[21] I. Alkorta, I. Rozas, J. Elguero, J. Chem. Soc. Rev. 27 (1998) 163.
[22] R. Custelcean, J.E. Jackson, Chem. Rev. 101 (2001) 1963.
[23] (a) R.G. Kultyshev, J. Liu, E.A Meyers, S.G. Shore, Inorg. Chem. 39 (2000) 3333–3341;
(b) M. Davidson, A.K. Hughes, T.B Marder, K. Wade (Eds.), Contemporary Boron Chemistry, Royal Society of Chemistry, Cambridge, England, 2000, pp. 166–170.
[24] For in-depth analyses of C–H···π interactions see: M. Nishio, M. Hirota, Y. Umezawa, The CH/π Interaction (Evidence, Nature and Consequences), Wiley-VCH, New York, 1998.
[25] (a) M.J. Potrezebowski, M. Michalska, A.E. Koziol, S. Kazmierski, T. Lis, J. Pluskowski, W. Ciesielski, J. Org. Chem. 63 (1998) 4209;
(b) H. Borrmann, I. Persson, M. Sangström, C.M.V. Ståhlhandske, J. Chem. Soc. Perkin Trans. 2 (2000) 393.
[26] M.G.S. Londesborough, C. Price, M. Thornton-Pett, W. Clegg, J.D. Kennedy, Chem. Commun. (1999) 298.
[27] R.J. Pace, J. Williams, R.L. Williams, J. Chem. Soc. (1961) 2196.
[28] J. Bould, U. Dörfler, M. Thornton-Pett, J.D. Kennedy, Inorg. Chem. Commun. 4 (2001) 546.
[29] (a) M.F. Hawthorne, A.R. Pitochelli, J Am. Chem. Soc. 81 (1959) 5519;
(b) M.F. Hawthorne, R.L. Pilling, R.N. Grimes, J. Am. Chem. Soc. 86 (1964) 5338;
(c) M.F. Hawthorne, R.L. Pilling, Inorg. Synth. 9 (1967) 16.
[30] D. Seyferth, W.S. Rees, Jr., Chem. Mater. 3 (1991) 1106.
[31] A.L. Spek, Acta Crystallogr. Sect. A 46 (1990) C34.
[32] G.A. Jeffrey, W. Saenger, Hydrogen Bonding in Biological Structures, 2nd ed., Springer, New York, 1994.